Astrometric positions for 18 irregular satellites of giant planets from 23 years of observations[,★,★★,★★★,★★★★]

A. R. Gomes-Júnior[1], M. Assafin[1,†], R. Vieira-Martins[1,2,3,‡], J.-E. Arlot[4], J. I. B. Camargo[2,3], F. Braga-Ribas[2,5], D. N. da Silva Neto[6], A. H. Andrei[1,2,§], A. Dias-Oliveira[2], B. E. Morgado[1], G. Benedetti-Rossi[2], Y. Duchemin[4,7], J. Desmars[4], V. Lainey[4], W. Thuillot[4]

[1] Observatório do Valongo/UFRJ, Ladeira Pedro Antônio 43, CEP 20.080-090 Rio de Janeiro - RJ, Brazil
e-mail: `altair08@astro.ufrj.br`
[2] Observatório Nacional/MCT, R. General José Cristino 77, CEP 20921-400 Rio de Janeiro - RJ, Brazil
e-mail: `rvm@on.br`
[3] Laboratório Interinstitucional de e-Astronomia - LIneA, Rua Gal. José Cristino 77, Rio de Janeiro, RJ 20921-400, Brazil
[4] Institut de mécanique céleste et de calcul des éphémérides - Observatoire de Paris, UMR 8028 du CNRS, 77 Av. Denfert-Rochereau, 75014 Paris, France
e-mail: `arlot@imcce.fr`
[5] Federal University of Technology - Paraná (UTFPR / DAFIS), Rua Sete de Setembro, 3165, CEP 80230-901, Curitiba, PR, Brazil
[6] Centro Universitário Estadual da Zona Oeste, Av. Manual Caldeira de Alvarenga 1203, CEP 23.070-200 Rio de Janeiro RJ, Brazil
[7] ESIGELEC-IRSEEM, Technopôle du Madrillet, Avenue Galilée, 76801 Saint-Etienne du Rouvray, France

Received: ; accepted:

ABSTRACT

Context. The irregular satellites of the giant planets are believed to have been captured during the evolution of the solar system. Knowing their physical parameters, such as size, density, and albedo is important for constraining where they came from and how they were captured. The best way to obtain these parameters are observations in situ by spacecrafts or from stellar occultations by the objects. Both techniques demand that the orbits are well known.
Aims. We aimed to obtain good astrometric positions of irregular satellites to improve their orbits and ephemeris.
Methods. We identified and reduced observations of several irregular satellites from three databases containing more than 8000 images obtained between 1992 and 2014 at three sites (Observatório do Pico dos Dias, Observatoire de Haute-Provence, and European Southern Observatory - La Silla). We used the software PRAIA (Platform for Reduction of Astronomical Images Automatically) to make the astrometric reduction of the CCD frames. The UCAC4 catalog represented the International Celestial Reference System in the reductions. Identification of the satellites in the frames was done through their ephemerides as determined from the SPICE/NAIF kernels. Some procedures were followed to overcome missing or incomplete information (coordinates, date), mostly for the older images.
Results. We managed to obtain more than 6000 positions for 18 irregular satellites: 12 of Jupiter, 4 of Saturn, 1 of Uranus (Sycorax), and 1 of Neptune (Nereid). For some satellites the number of obtained positions is more than 50% of what was used in earlier orbital numerical integrations.
Conclusions. Comparison of our positions with recent JPL ephemeris suggests there are systematic errors in the orbits for some of the irregular satellites. The most evident case was an error in the inclination of Carme.

Key words. Astrometry - Planets and satellites: general - Planets and satellites: individual: Jovian and Saturnian irregular satellites

1. Introduction

The irregular satellites of the giant planets are smaller than the regular moons, having more eccentric, inclined, distant, and in most cases, retrograde orbits. Owing to their orbital configurations, it is largely accepted that these objects were captured in the early solar system (Sheppard & Jewitt 2003).

Because they are faint, the majority of these objects were only discovered in the last century[1] . They were never visited by a spacecraft, with the exception of Himalia, Phoebe and Nereid, in a flyby by the Cassini space probe in 2000 for Himalia (Porco et al. 2003) and in 2004 for Phoebe (Desmars et al. 2013) and in a flyby by the Voyager 2 space probe in 1989 for Nereid (Smith et al. 1989). Even in situ, they were still opportunity target obser-

[1] Website: http://ssd.jpl.nasa.gov/?sat_discovery

vations resulting in not optimal measurements, with size errors of $10km$ for Himalia and $25km$ for Nereid (Thomas et al. 1991). The exception is Phoebe with a very accurate measurement of size with a mean radius error of $0.7km$ (Thomas 2010).

If these objects were captured, there remains the question of where they came from. Clark et al. 2005 show from imaging spectroscopy from Cassini that Phoebe has a surface probably covered by material from the outer solar system and Grav et al. 2003 show that the satellites of the Jovian Prograde Group Himalia have gray colors implying that their surfaces are similar to that of C-type asteroids. In that same work, the Jovian Retrograde Group Carme was found to have surface colors similar to the D-type asteroids as for the Hilda or Trojan families, while JXIII Kalyke has a redder color like Centaurs or trans-Neptunian objects (TNOs).

For Saturnian satellites, Grav & Bauer 2007 show by their colors and spectral slopes that these satellites contain a more or less equal fraction of C-, P-, and D-like objects, but SXXII Ijiraq is marginally redder than D-type objects. These works may suggest different origins for the irregular satellites.

In this context, we used three databases for deriving precise positions for the irregular satellites observed at the Observatório do Pico dos Dias (1.6 m and 0.6 m telescopes, IAU code 874), the Observatoire Haute-Provence (1.2m telescope, IAU code 511), and ESO (2.2 m telescope, IAU code 809). Many irregular satellites were observed between 1992 and 2014, covering a few orbital periods of these objects (12 satellites of Jupiter, 4 of Saturn, Sycorax of Uranus, and Nereid of Neptune).

Since their ephemerides are not very precise, predicting and observing stellar occultations are very difficult, and no observation of such an event for an irregular satellite is found in the literature. The precise star positions to be derived by the ESA astrometry satellite Gaia (de Bruijne 2012) will render better predictions with the only source of error being the ephemeris. The positions derived from our observations can be used in new orbital numerical integrations, generating more precise ephemerides.

The power of stellar occultations for observing relatively small diameter solar system objects is supported by recent works, such as the discovery of a ring system around the Centaur (10199) Chariklo (Braga-Ribas et al. 2014). Once irregular satellites start to be observed by this technique, it will be possible to obtain their physical parameters (shape, size, albedo, density) with unprecedented precision. For instance, in this case, sizes could be obtained with kilometer accuracy. The knowledge of these parameters would in turn bring valuable information for studying the capture mechanisms and origin of the irregular satellites.

The databases are described in Sect. 2. The astrometric procedures in Sect. 3. The obtained positions are presented in Sect 4 and analyzed in Sect. 5. Conclusions are given in Sect. 6.

2. Databases

Our three databases consist of optical CCD images from many observational programs performed with different telescopes and detectors that target a variety of objects, among which are irregular satellites. The observations were made at three sites: Observatório do Pico dos Dias (OPD), Observatoire Haute-Provence (OHP), and the European Southern Observatory (ESO). All together there are more than 8000 FITS images obtained in a large time span (1992-2014) for the irregular satellites. Since the OHP and mostly the OPD database registers were not well organized, we had to start from scratch and develop an automatic procedure

to identify and filter only the images of interest, that is, for the irregular satellites. The instrument and image characteristics are described in the following sections.

2.1. OPD

The OPD database was produced at the Observatório do Pico dos Dias (OPD, IAU code 874, 45° 34′ 57″ W, 22° 32′ 04″ S, 1864 m)[2], located at geographical longitude , in Brazil. The observations were made between 1992 and 2014 by our group in a variety of observational programs. Two telescopes of 0.6 m diameter (Zeiss and Boller & Chivens) and one 1.6 m diameter (Perkin-Elmer) were used for the observations. Identified were 5248 observations containing irregular satellites, with 3168 from the Boller & Chivens, 1967 from the Perkin-Elmer, and 113 from the Zeiss.

This is an inhomogeneous database with observations made with nine different detectors (see Table 1) and six different filters. The headers of most of the older FITS images had missing, incomplete, or incorrect coordinates or dates. In some cases, we could not identify the detector's origin. The procedures used to overcome these problems are described in Sect. 3.

Table 1. Characteristics of OPD detectors used in this work.

Perkin-Elmer		
Detector	Image size (pixel)	Pixel Scale (μm/px)
CCD048	770 x 1152	22.5
CCD098	2048 x 2048	13.5
CCD101	1024 x 1024	24.0
CCD105	2048 x 2048	13.5
CCD106	1024 x 1024	24.0
CCD301	385 x 578	22.0
CCD523	455 x 512	19.0
IKON	2048 x 2048	13.5
IXON	1024 x 1024	13.5

The plate scale of the telescopes are 13.09"/mm for Perkin-Elmer, 25.09"/mm for Boller & Chivens and 27.5"/mm for Zeiss.

2.2. OHP

The instrument used at the Observatoire de Haute Provence (OHP, IAU code 511, 5° 42′ 56.5″ E, 43° 55′ 54.7″N, 633.9 m)[3] was the 1.2m-telescope in a Newton configuration. The focal length is 7.2 m. The observations were made between 1997 and 2008. During this time only one CCD detector 1024×1024 was used. The size of field is $12' \times 12'$ with a pixel scale of $0.69''$. From these observations, 2408 were identified containing irregular satellites.

2.3. ESO

Observations were made at the 2.2 m Max-Planck ESO (ESO2p2) telescope (IAU code 809, 70°44′1.5″ W, 29°15′31.8″ S, 2345.4 m)[4] with the Wide Field Imager (WFI) CCD mosaic detector. Each mosaic is composed of eight CCDs of $7.5' \times 15'$ (α, δ) sizes, resulting in a total coverage of $30' \times 30'$ per mosaic.

Each CCD has $4k \times 2k$ pixels with a pixel scale of 0.238″. The filter used was a broad-band R filter (ESO#844) with $\lambda_c = 651.725$ nm and $\Delta\lambda = 162.184$ nm. The telescope was shifted between exposures in such a way that each satellite was observed at least twice in different CCDs.

The satellites were observed in 24 nights, divided in five runs between April 2007 and May 2009 in parallel with, and using the same observational and astrometric procedures of the program that observed stars along the sky path of trans-Neptunian objects (TNOs) to identify candidates for stellar occultation (see Assafin et al. 2010, 2012). A total of 810 observations were obtained for irregular satellites.

3. Astrometry

Almost all the frames were photometrically calibrated with auxiliary bias and flat-field frames by means of standard procedures using IRAF[5] and, for the mosaics, using the esowfi (Jones & Valdes 2000) and mscred (Valdes 1998) packages. Some of the nights at OPD did not have bias and flat-field images so the correction was not possible.

The astrometric treatment was made with the Platform for Reduction of Astronomical Images Automatically (PRAIA) (Assafin et al. 2011). The (x, y) measurements were performed with two-dimensional circular symmetric Gaussian fits within one full width half maximum (FWHM = seeing). Within one FWHM, the image profile is described well by a Gaussian profile, which is free of the wing distortions, which may jeopardize the determination of the center. PRAIA automatically recognizes catalog stars and determines (α, δ) with a user-defined model relating the (x, y) measured and (X, Y) standard coordinates projected in the sky tangent plane.

We used the UCAC4 (Zacharias et al. 2013) as the practical representative of the International Celestial Reference System (ICRS). For each frame, we used the six constants polynomial model to relate the (x, y) measurements with the (X, Y) tangent plane coordinates. For ESO, we followed the same astrometric procedures as described in detail in Assafin et al. (2012); the (x, y) measurements of the individual CCDs were precorrected by a field distortion pattern, and all positions coming from different CCDs and mosaics were then combined using a third degree polynomial model to produce a global solution for each night and field observed, and final (α, δ) object positions were obtained in the UCAC4 system.

In Table 2 we list the average mean error in α and δ for the reference stars obtained by telescope, the average (x, y) measurement errors of the Gaussian fits described above, and the mean number of UCAC4 stars used by frame. For all databases, about 20% of outlier reference stars were eliminated for presenting (O-C) position residuals higher than 120 mas in the (α, δ) reductions.

To help identify the satellites in the frames and derive the ephemeris for the instants of the observations for comparisons (see Sect 5), we used the kernels from SPICE/JPL[6]. Emelyanov & Arlot (2008) and references therein also provided ephemeris of similar quality for the irregular satellites. For instance, for Himalia, which has relatively good orbit solutions, the ephemerides differ by less than 20 *mas*, and in the case of less-known orbits, like Ananke, the differences are less than 90 *mas*. We chose to use the JPL ephemeris because they used more recent observations (see Jacobson et al. 2012). The JPL

---

[5] Website: http://iraf.noao.edu/
[6] Website: http://naif.jpl.nasa.gov/naif/toolkit.html

Table 2. Astrometric (α, δ) reduction by telescope.

| Telescope | Mean errors | | UCAC4 stars | Gaus. errors | |
	σ_α mas	σ_δ mas		x mas	y mas
PE(OPD)	51	48	24	15	15
B&C (OPD)	56	55	36	29	29
Zeiss (OPD)	58	57	95	26	26
OHP	50	49	46	26	26
ESO	26	25	632	15	15

Mean errors are the standard deviations in the (O−C) residuals from (α, δ) reductions with the UCAC4 catalog. Gaussian errors are the errors in the Gaussian fit used to perform the (x, y) measurements.

ephemeris that represented the Jovian satellites in this work was the DE421 + JUP300. For the Saturnian satellites, the ephemeris was DE421 + SAT359 to Hyperion, Iapetus, and Phoebe and DE421 + SAT361 to Albiorix, Siarnaq, and Paaliaq. The DE421 + URA095 was used for Sycorax and DE421 + NEP081 for Nereid. More recent JPL ephemeris versions became available after completion of this work, but this did not affect the results.

In the OPD database, there were some images (mostly the older ones) with missing coordinates or the wrong date in their headers. In the case of missing or incorrect coordinates, we adopted the ephemeris as the central coordinates of the frames. When the time was not correct, the FOV identification failed. In this case, a search for displays of wrong date (year) was performed. Problems like registering local time instead of UTC were also identified and corrected.

In all databases, for each night a sigma-clipping procedure was performed to eliminate discrepant positions (outliers). A threshold of 120 mas and a deviation of more than 2.5 sigma from the nightly average ephemeris offsets were adopted.

From Tables 3 to 7 we list the average dispersion (standard deviation) of the position offsets with regard to the ephemeris for α and δ obtained by telescope for each satellite. The final number of frames, number of nights (in parenthesis), the mean number of UCAC4 stars used in the reduction and the approximate V magnitude are also given. The dashed lines separate the satellites from different families with similar orbital parameters: Himalia Group (Himalia, Elara, Lysithea and Leda), Pasiphae Group (Pasiphae, Callirrhoe and Megaclite), and Ananke Group (Ananke and Praxidike). Carme and Sinope are the only samples of their groups. From Saturn, Siarnaq and Paaliaq are from the Inuit Group while Phoebe and Albiorix are the only samples in their groups.

The differences in the dispersion of the ephemeris offsets of the same satellite for distinct telescopes seen in Tables 3 to 7 are caused by the different distribution of observations along the orbit for each telescope. This can be seen in Fig. 1 for Carme and Fig. 2 for Pasiphae and for all objects in the online material. Since the observations cover different segments of the orbit, the dispersion of the offsets may vary for different telescopes for a single satellite, with larger covered segments usually implying larger dispersions and vice versa. For Nereid, due to its high eccentric orbit, the observations are located between 90° and 270° of true anomaly where Nereid remains most of the time.

No solar phase correction was applied to the positions. For the biggest irregular satellite of Jupiter, Himalia, it was verified that the maximum deviation in the position due to phase angle is 1.94 *mas* using the phase correction described in Lindegren (1977). For the other satellites, which are smaller objects, this

Table 3. Astrometric (α, δ) reduction for each satellite observed with the Perkin-Elmer telescope.

| Satellite | Offsets (sigma) | | Nr | UCAC4 | |
	σ_α mas	σ_δ mas	frames (nights)	stars	Mag
Himalia	290	45	238 (18)	37	14
Elara	230	118	99 (12)	32	16
Lysithea	107	79	53 (8)	41	18
Leda	207	79	6 (2)	46	19
Pasiphae	157	92	144 (13)	22	17
Callirrhoe	66	35	9 (1)	3	21
Carme	97	94	68 (7)	49	18
Sinope	155	77	37 (8)	42	18
Ananke	93	185	52 (7)	40	19
Phoebe	73	95	410 (22)	6	16
Nereid	200	142	289 (29)	8	19

The offsets (sigma) are the average standard deviations of the ephemeris offsets from the (α, δ) positions of the satellites. Also given are the approximate satellite V magnitude and the average number of UCAC4 reference stars per frame.

Table 4. Astrometric (α, δ) reduction for each satellite observed with the Boller & Chivens telescope.

| Satellite | Offsets (sigma) | | Nr | UCAC4 | |
	σ_α mas	σ_δ mas	frames (nights)	stars	Mag
Himalia	83	43	560 (31)	57	14
Elara	55	43	294 (23)	53	16
Lysithea	23	42	7 (2)	60	18
Pasiphae	128	71	140 (14)	57	17
Carme	68	111	22 (4)	45	18
Sinope	59	17	4 (1)	22	18
Phoebe	43	48	810 (42)	17	16
Nereid	61	45	514 (38)	20	19

Same as in Table 3.

Table 5. Astrometric (α, δ) reduction for each satellite observed with the Zeiss telescope.

| Satellite | Offsets (sigma) | | Nr | UCAC4 | |
	σ_α mas	σ_δ mas	frames (nights)	stars	Mag
Himalia	112	72	56 (4)	91	14
Elara	17	21	10 (1)	146	16
Pasiphae	24	25	11 (1)	140	17
Phoebe	37	30	19 (1)	16	16

Same as in Table 3.

deviation is even smaller. Since our position error is one order of magnitude higher, this effect was neglected.

4. Satellite positions

The final set of positions of the satellites consists in 6523 cataloged positions observed between 1992 and 2014 for 12 satellites of Jupiter, 4 of Saturn, 1 of Uranus, and 1 of Neptune. The topocentric positions are in the ICRS. The catalogs (one for each satellite) contain epoch of observations, the position error, filter used, estimated magnitude (from PSF fitting) and telescope origin. The magnitude errors can be as high as 1 mag; they are not photometrically calibrated and should be used with care. The po-

Table 6. Astrometric (α, δ) reduction for each satellite observed with the OHP telescope.

| Satellite | Offsets (sigma) | | Nr | UCAC4 | |
	σ_α mas	σ_δ mas	frames (nights)	stars	Mag
Himalia	49	66	357 (43)	49	14
Elara	52	61	187 (25)	37	16
Lysithea	63	50	84 (13)	56	18
Leda	118	33	48 (7)	14	19
Pasiphae	101	75	248 (32)	39	17
Carme	114	96	204 (29)	39	18
Sinope	196	73	169 (25)	43	18
Ananke	100	89	141 (20)	62	19
Phoebe	30	31	516 (63)	51	16
Siarnaq	46	98	20 (6)	32	20

Same as in Table 3.

Table 7. Astrometric (α, δ) reduction for each satellite observed with the ESO telescope.

| Satellite | Offsets (sigma) | | Nr | UCAC4 | |
	σ_α mas	σ_δ mas	frames (nights)	stars	Mag
Himalia	76	74	23 (2)	1153	14
Elara	112	87	46 (4)	1492	16
Lysithea	76	88	90 (6)	695	18
Leda	60	125	44 (3)	632	19
Pasiphae	70	114	66 (5)	836	17
Callirrhoe	29	33	16 (1)	493	21
Megaclite	52	34	10 (1)	445	22
Ananke	225	19	57 (3)	761	18
Praxidike	7	38	2 (1)	1934	21
Carme	140	110	37 (4)	1074	18
Sinope	339	70	11 (2)	1542	18
Themisto	894	28	16 (2)	1232	21
Phoebe	102	57	32 (5)	312	16
Siarnaq	86	66	56 (6)	283	20
Paaliaq	301	59	11 (4)	382	21
Albiorix	76	50	46 (6)	330	20
Sycorax	150	82	35 (9)	375	21
Nereid	115	78	99 (12)	362	19

Same as in Table 3.

sition errors were estimated from the dispersion of the ephemeris offsets of the night of observation of each position. Thus, these position errors are probably overestimated because there must be ephemeris errors present in the dispersion of the offsets. These position catalogs are freely available in electronic form at the CDS (see a sample in Table 8) and at the IAU NSDC data base at www.imcce.fr/nsdc.

The number of positions acquired is significant compared to the number used in the numerical integration of orbits by the JPL (Jacobson et al. 2012) as shown in Table 9.

5. Comparison with ephemeris

Intending to see the potential of our results to improve the orbit of the irregular satellites observed, we analyzed the offsets of our positions with regard to the ephemeris mentioned in Sect. 3. Taking Carme as example, we plot the mean ephemeris offsets for each night in Fig. 1 and their dispersions (one sigma error bars) as a function of the true anomaly in right ascension (1a)

Table 8. CDS data table sample for Himalia.

RA (ICRS) Dec			RA error	Dec error	Epoch	Mag	Filter	Telescope	IAU code
h m s	° ′ ″		(mas)	(mas)	(jd)				
16 59 11.6508	-22 00 44.855		17	12	2454147.78241319	16.0	C	BC	874
16 59 11.6845	-22 00 44.932		17	12	2454147.78332384	15.8	C	BC	874
16 59 11.7181	-22 00 44.978		17	12	2454147.78422477	16.0	C	BC	874
16 59 11.7818	-22 00 45.143		17	12	2454147.78602662	15.9	C	BC	874
16 59 11.8188	-22 00 45.232		17	12	2454147.78693750	16.0	C	BC	874
17 17 11.0344	-22 47 19.415		30	24	2454205.63885463	16.1	U	BC	874
17 17 11.0270	-22 47 19.381		30	24	2454205.63959167	16.1	U	BC	874
17 17 11.0258	-22 47 19.366		30	24	2454205.64031875	16.1	U	BC	874
17 17 11.0192	-22 47 19.417		30	24	2454205.64104583	16.1	U	BC	874

This sample corresponds to 9 observations of Himalia from February 16, 2007 and April 15, 2007. Tables contain the topocentric ICRS coordinates of the irregular satellites, the position error estimated from the dispersion of the ephemeris offsets of the night of observation, the UTC time of the frame's mid-exposure in Julian date, the estimated magnitude, the filter used, the telescope origin and correspondent IAU code. The filters may be U, B, V, R or I following the Johnson system; C stands for clear (no filter used), resulting in a broader R band magnitude, RE for the broad-band R filter ESO#844 with λ_c = 651.725 nm and $\Delta\lambda$ = 162.184 nm (full width at half maximum) and "un" for unknown filter. E, OH, PE, BC and Z stand for the ESO, OHP, Perkin-Elmer, Bollen & Chivens and Zeiss telescopes, respectively.

Table 9. Comparison between the number of positions obtained in our work with the number used in the numerical integration of orbits by the JPL as published by Jacobson et al. 2012.

Satellite	Number of Positions				
	OPD	OHP	ESO	Total	Jacobson
Himalia	854	357	23	1234	1757
Elara	403	187	46	636	1115
Lysithea	60	84	90	234	431
Leda	6	48	44	98	178
Pasiphae	295	248	66	609	1629
Callirrhoe	9	-	16	25	95
Megaclite	-	-	10	10	50
Ananke	52	141	57	250	600
Praxidike	-	-	2	2	59
Carme	90	204	37	331	973
Sinope	41	169	11	221	854
Themisto	-	-	16	16	55
Phoebe	1239	516	32	1787	3479
Siarnaq	-	20	56	76	239
Paaliaq	-	-	11	11	82
Albiorix	-	-	46	46	137
Sycorax	-	-	35	35	237
Nereid	803	-	99	902	716

and declination (1b). Figure 1b clearly shows a systematic error in declination. When Carme is close to its apojove (true anomaly = 180°), its offsets are more likely to be more negative than those close to its perijove (true anomaly = 0°). The offsets obtained from observations by four telescopes using different cameras and filters are in good agreement, meaning that there is an error in the ephemeris of Carme, most probably due to an error in its orbital inclination.

This pattern in declination was also seen for other satellites like Pasiphae (Fig: 2) and Ananke (plots for other satellites with significant number of observations can be seen in the online material). For some satellites, the orbital coverage is not enough to clearly indicate the presence of systematic errors in specific orbital elements. However, after comparing the internal position mean errors of the reductions (Table 2) with the external position errors estimated from the dispersion of the ephemeris off-

sets (Tables 3 to 7), we see position error values that are much higher than expected from the mean errors. This means that besides some expected astrometric errors, significant ephemeris errors must also be present.

6. Conclusions

We managed a large database with FITS images acquired by five telescopes in three sites between 1992 and 2014. From that, we identified 8466 observations of irregular satellites, from which we managed to obtain 6523 suitable astrometric positions, giving a total of 3666 positions for 12 satellites of Jupiter, 1920 positions for 4 satellites of Saturn, 35 positions for Sycorax (Uranus) and 902 positions for Nereid (Neptune).

The positions of all the objects were determined using the PRAIA package. The package was suited to coping with the huge number of observations and with the task of identifying the satellites within the database. PRAIA tasks were also useful for dealing with the missing or incorrect coordinate and time stamps present mostly in the old observations.

The UCAC4 was used as the reference frame. Based on the comparisons with ephemeris, we estimate that the position errors are about 60 mas to 80 mas depending on the satellite brightness. For some satellites the number of positions obtained in this work is comparable to the number used in the numerical integration of orbits by the JPL (Jacobson et al. 2012) (see Table 9). For instance, the number of new positions for Himalia is about 70% of the number used in the numerical integation of orbits by JPL. Systematic errors in the ephemeris were found for at least some satellites (Ananke, Carme, Elara and Pasiphae). In the case of Carme, we showed an error in the orbital inclination (see Fig. 1).

The positions derived in this work can be used in new orbital numerical integrations, generating more precise ephemerides. Stellar occultations by irregular satellites could then be predicted better. Based on this work, our group has already computed occultation predictions for the eight major irregular satellites of Jupiter. These predictions will be published in a forthcoming paper.
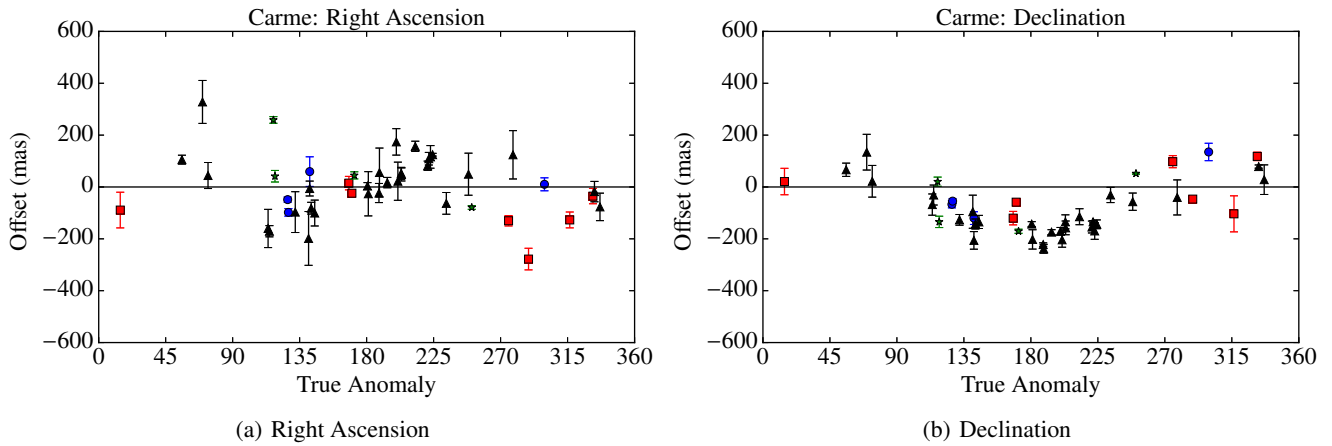
(a) Right Ascension

(b) Declination

Fig. 1. Mean ephemeris offsets and dispersions (1 sigma error bars) in the coordinates of Carme taken night by night by true anomaly for each telescope. The red square is for the observations with the Perkin-Elmer telescope from OPD, the blue circle for Boller & Chivens, the magenta triangle down for Zeiss, the black triangle up for OHP and the green star for ESO.
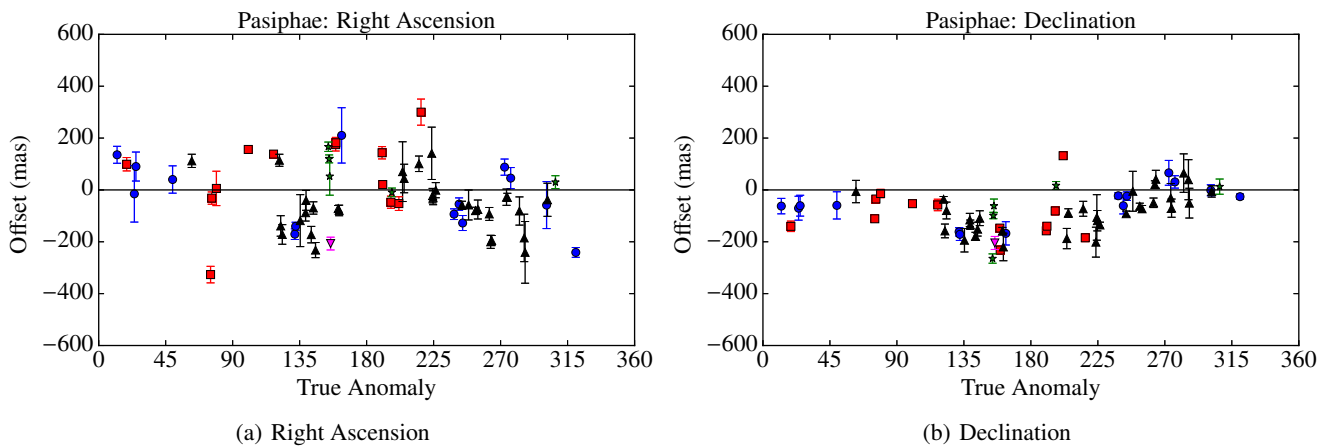

(a) Right Ascension

(b) Declination

Fig. 2. Same as in Fig 1 for Pasiphae.

References

Assafin, M., Camargo, J. I. B., Vieira Martins, R., et al. 2010, Astronomy and Astrophysics, 515, A32

Assafin, M., Camargo, J. I. B., Vieira Martins, R., et al. 2012, Astronomy and Astrophysics, 541, A142

Assafin, M., Vieira Martins, R., Camargo, J. I. B., et al. 2011, in Gaia follow-up network for the solar system objects : Gaia FUN-SSO workshop proceedings, held at IMCCE -Paris Observatory, France, November 29 - December 1, 2010. ISBN 2-910015-63-7, ed. P. Tanga & W. Thuillot, 85–88

Braga-Ribas, F. et al. 2014, Nature, 72

Clark, R. N. et al. 2005, Nature, 435, 66

de Bruijne, J. H. J. 2012, Ap&SS, 341, 31

Desmars, J. et al. 2013, Astronomy and Astrophysics, 553

Emelyanov, N. V. & Arlot, J.-E. 2008, Astronomy and Astrophysics, 487, 759–765

Grav, T. & Bauer, J. 2007, Icarus, 191, 267

Grav, T., Holman, M. J., Gladman, B. J., & Aksnes, K. 2003, Icarus, 166, 33

Jacobson, R. et al. 2012, The Astronomical Journal, 144, 8 pgs

Jones, H. & Valdes, F. 2000, in "Handling ESO WFI Data With IRAF", ESO Document number 2p2-MAN-ESO-22200-00002

Lindegren, L. 1977, Astronomy and Astrophysics, 57, 55

Porco, C. et al. 2003, Science, 299, 1541

Sheppard, S. S. & Jewitt, D. C. 2003, Nature, 423, 261

Smith, B. A. et al. 1989, Science, 246, 1422

Thomas, P. 2010, Icarus, 208, 395

Thomas, P., Veverka, J., & Helfenstein, P. 1991, Journal of Geophysical Research: Space Physics, 96, 19253

Valdes, F. G. 1998, in "The IRAF Mosaic Data Reduction Package" in Astronomical Data Analysis Software and Systems VII, A.S.P. Conference Ser., Vol 145, eds R. Albrecht, R. N. Hook and H. A. Bushouse, 53

Zacharias, N., Finch, C. T., Girard, T. M., et al. 2013, AJ, 145, 44

Appendix A: Ephemeris offsets as a function of true anomaly for all observed irregular satellites

The distribution of ephemeris offsets along the orbit of the satellites are shown below. The red square is for the observations with the Perkin-Elmer telescope from OPD, the blue circle for Boller & Chivens, the magenta triangle down for Zeiss, the black triangle up for OHP and the green star for ESO. For Carme and Pasiphae see Figs. 1 and 2 in Section 5.
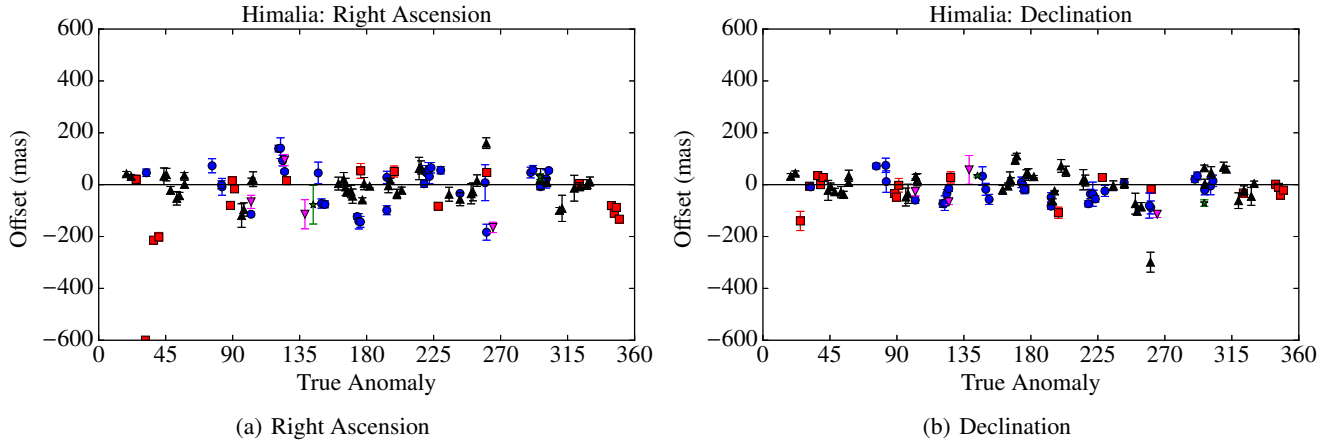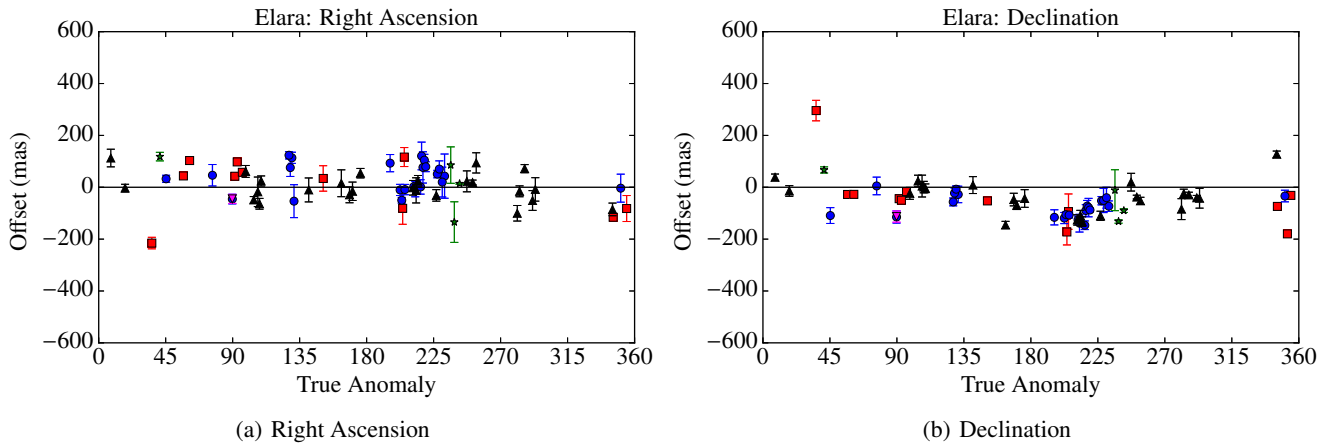

(a) Right Ascension

(b) Declination

Fig. A.1. Mean ephemeris offset and dispersion (1 sigma error bars) in the coordinates of Himalia taken night by night as a function of true anomaly.

(a) Right Ascension

(b) Declination

Fig. A.2. Same as in Fig A.1 for Elara.

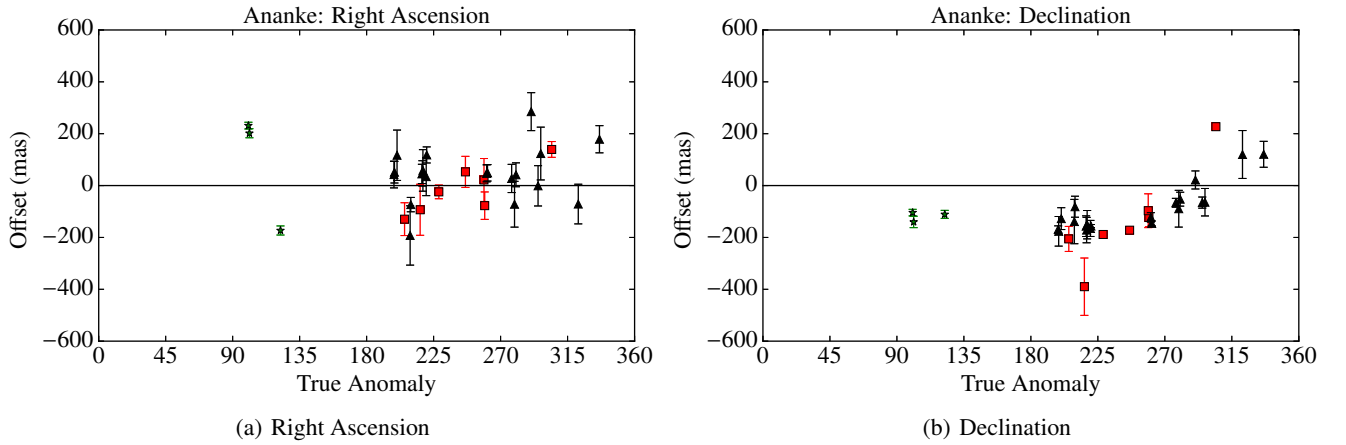

(a) Right Ascension

(b) Declination
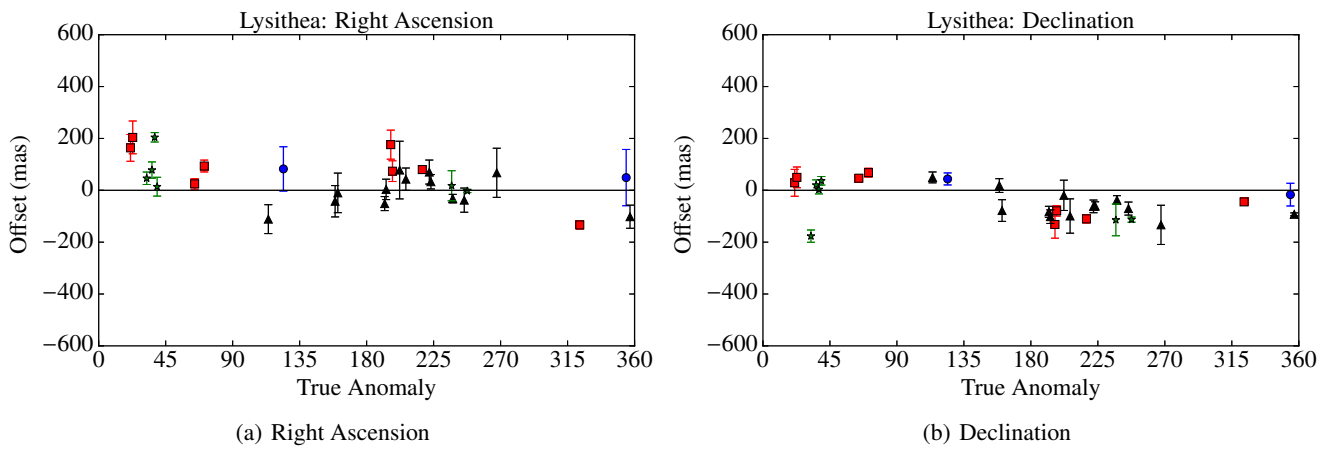
Fig. A.3. Same as in Fig A.1 for Lysithea.
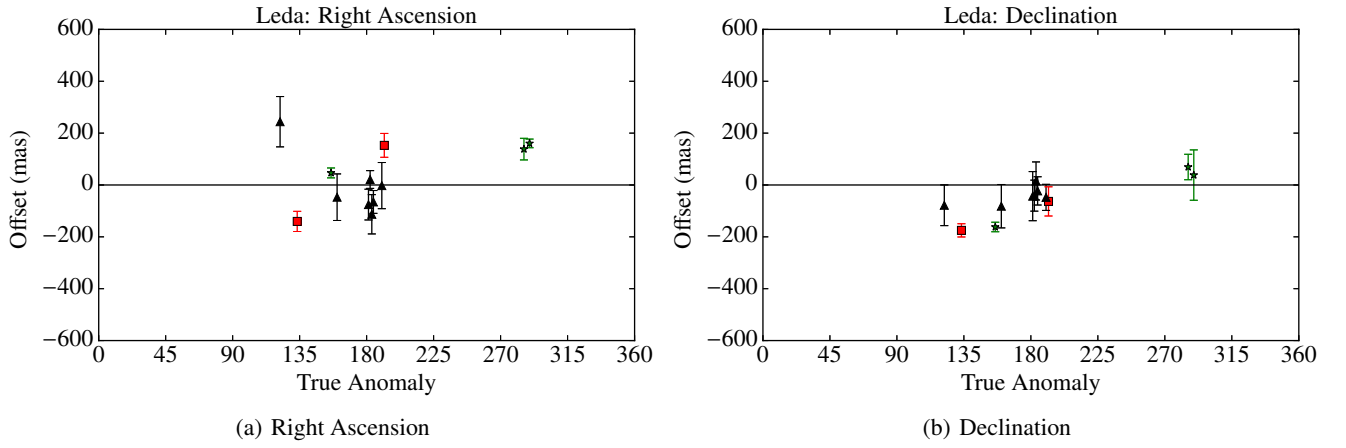
Fig. A.4. Same as in Fig A.1 for Leda.

(a) Right Ascension

(b) Declination
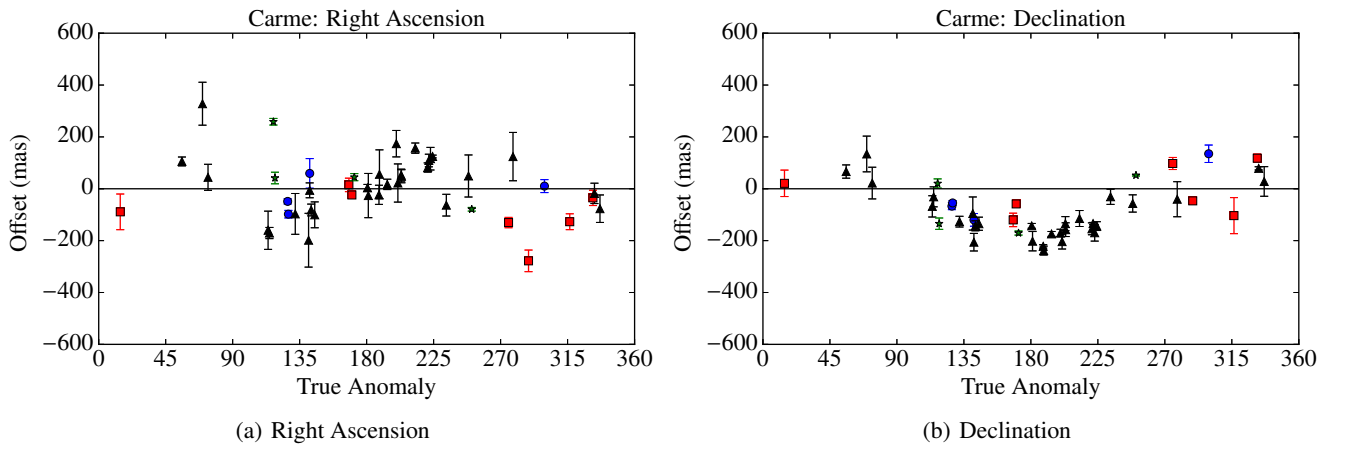
Fig. A.5. Same as in Fig A.1 for Carme.

(a) Right Ascension

(b) Declination

Fig. A.6. Same as in Fig A.1 for Ananke.

(a) Right Ascension

(b) Declination
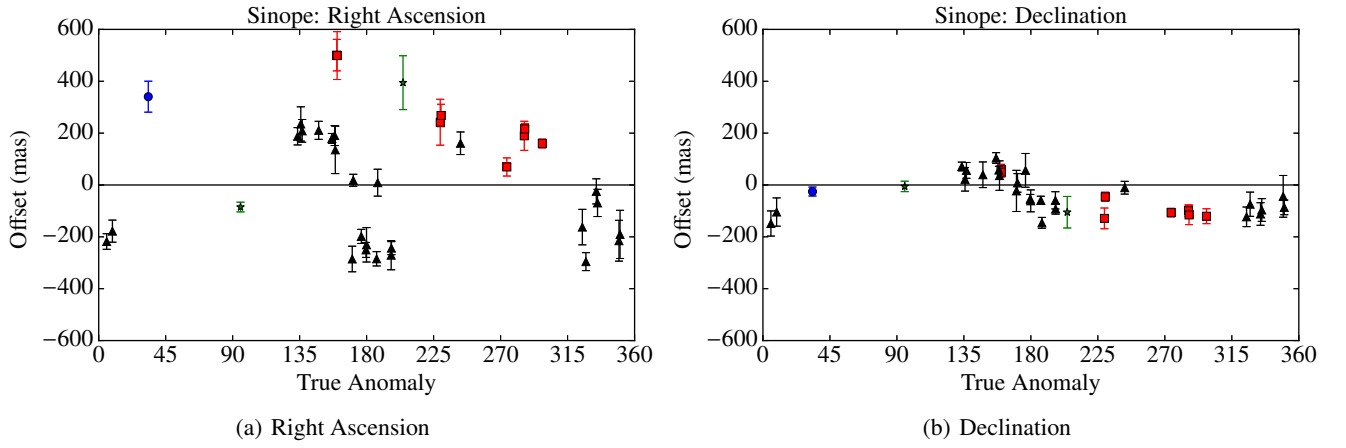
Fig. A.7. Same as in Fig A.1 for Sinope.
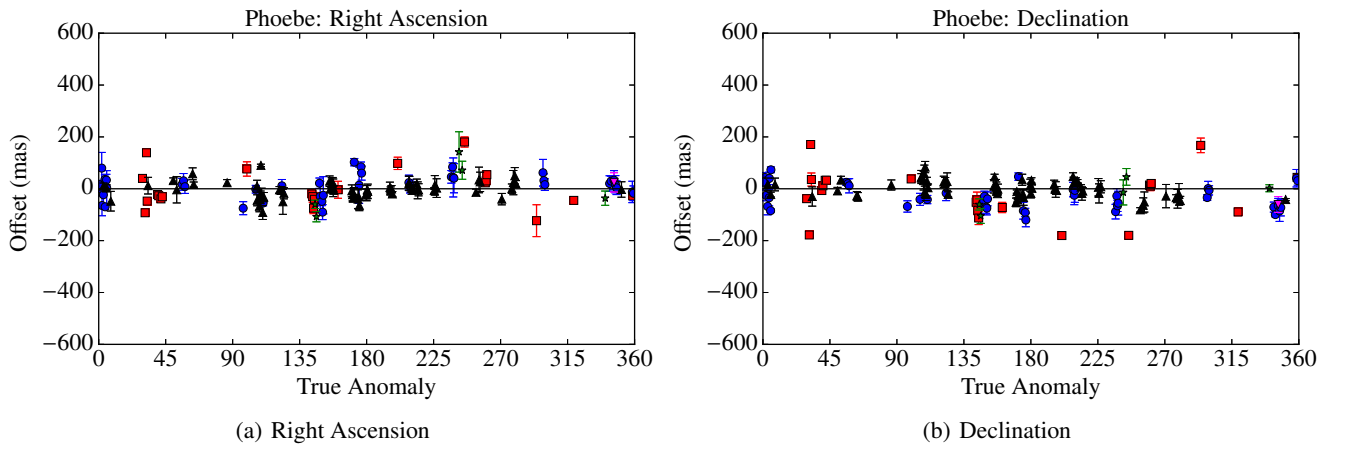
Fig. A.8. Same as in Fig A.1 for Phoebe.
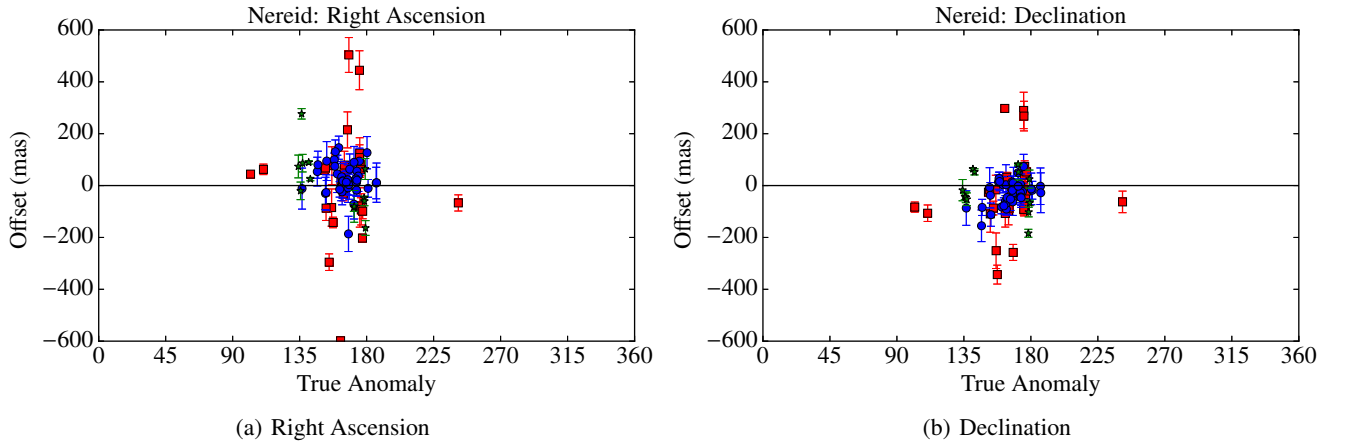
Fig. A.9. Same as in Fig A.1 for Nereid.